

# Design and Optimization of Gasketed-Plate Heat Exchanger using Bees Algorithm

**Navid Bozorgan**

Department of Mechanical Engineering, Dezful Branch, Islamic Azad University, Dezful, Iran

**Ashkan Ghafouri \***

Department of Mechanical Engineering, Ahvaz Branch, Islamic Azad University, Ahvaz, Iran

E-mail: a.ghafouri@iauahvaz.ac.ir

\*Corresponding author

**Ehsanolah Assareh**

Department of Mechanical Engineering,  
Dezful Branch, Islamic Azad University, Dezful, Iran

**Seyed Mohammad Safieddin Ardebili**

Department of Mechanical Engineering, Dezful Branch, Islamic Azad University, Dezful, Iran, and Department of Biosystems Engineering, Shahid Chamran University of Ahvaz, Ahvaz, Iran

**Received: 18 August 2020, Revised: 16 December 2020, Accepted: 20 December 2020**

**Abstract:** In the present study, the hydraulic-thermal design and optimization of a gasketed-plate heat exchanger (GPHE) with an objective function of heat exchanger performance index (the amount of transferred heat exchange to pumping power ratio) is carried out. This process is made by considering 6 design parameters (the port diameter, plate thickness, the enlargement factor, the compressed plate pack length, the horizontal port distance, and the vertical port distance) and through the Bees Algorithm (BA). The present study achieved three solution sets for the design parameters by investigating the sensitivity of the design parameters heeded in the optimization of the GPHE. The design parameters in these three optimal solution sets were opted for in such a way that heat transfer increased by 41.6%, 34.55%, and 20.7%, and pressure drop decreased by 11.89%, 27%, and 83%, respectively.

**Keywords:** Bees Algorithm, Design and Optimization, Gasketed-Plate Heat Exchanger, Heat Transfer Enhancement, Pressure Drop

**How to cite this paper:** Navid Bozorgan, Ashkan Ghafouri, Ehsanolah Assareh, and Seyed Mohammad Safieddin Ardebili, "Design and Optimization of Gasketed-Plate Heat Exchanger using Bees Algorithm", Int J of Advanced Design and Manufacturing Technology, Vol. 14/No. 3, 2021, pp. 55-64.  
DOI: 10.30495/admt.2021.1907203.1211

**Biographical notes:** **Navid Bozorgan** received his PhD from IAU University, Dezful branch, Iran in 2020. He is currently working on the improvement of the heat exchangers performance with the application of optimization algorithms. **Ashkan Ghafouri** is an Assistant Professor of Mechanical Engineering at IAU University-Ahvaz branch, Iran. He received his PhD in Mechanical Engineering from Urima University, Iran, in 2015. **Ehsanolah Assareh** is an Assistant Professor of Mechanical Engineering at IAU University-Dezful branch, Iran. He received his PhD in Mechanical Engineering from Semnan University, Iran, in 2016. **Seyed Mohammad Safieddin Ardebili** is currently instructor at Shahid Chamran University of Ahvaz. He received his PhD in Mechanical Engineering from Tarbiat Modares University, Iran, in 2014. His main research interest is working on multi-objective optimization coupled simulation analysis.

## 1 INTRODUCTION

Heat exchangers are widely utilized in engineering applications like chemical industries, electricity generation, food manufacturers, environmental engineering, energy recycling, air conditioning, and Refrigeration. Nowadays, considering the advancing technologies in the industrial processes, the demand for high performance and efficient heat exchangers is increasing. In recent studies, the optimization of geometric and process parameters to achieve the maximum performance and the least pressure drop in heat exchangers is aimed. This is made through the assessing the exchanger's relevant geometric, hydraulic, and thermal equations, and choosing the proper optimization algorithm as a novel approach for increasing the performance of heat exchangers, which is elaborated by the researchers [1-7].

Yin et al. [8] have implemented multi-objective optimization of a regenerative heat exchanger, mounted on the furnace shell, with the objective function of pressure drop and heat transfer level, entropy production, and with design parameters of tubes number, and the length and diameter of tubes through the genetic algorithm. The results demonstrate that the regenerative heat exchanger can decrease the heat exchange level and pressure drop by 18 percent, and 11 percent, respectively. Momeni et al. [9] have made the multi-objective optimization of marine diesel engine's air cooler with the objective function of total cost, exergy destruction ratio, and with parameters of tube outer diameter design, longitudinal and transverse pitch, the number of tube rows, fin pitch and the heat exchanger dimensions through the firefly algorithm. They have reported that the total cost, exergy destruction ratio, the air pressure drop are decreased by 4.03, 7.66, 12.4, and 2.95 percent.

Wu et al. [10] have optimized a spiral-wound heat exchanger by considering the thermal capacity at a constant rate and total transferred heat as the objective function, through the genetic algorithm. The angle of twist (in the range of 10 to 30 degrees), and spacer thickness (in the range of 0 to 10 mm), and the axial distance (in the range of 0 to 10 mm) are considered as the design parameters. The minimum total transferred heat in 4900.6 m<sup>2</sup> is decreased by 23.4 percent with an acceptable increase rate in pressure drop. The reported optimized angle of twist is 11.7 degrees, the spacer thickness is 0.00237 m and the axial distance between tubes is 0.00814 mm. Petinrin et al. [11] have performed the optimization of the preheater heat exchanger of the crude oil distillation unit (two shell and tube heat exchangers) by considering 13 design parameters in the specified ranges and by decreasing entropy to the minimum level through the firefly algorithm. The  $\epsilon$ -NTU and Delaware method are utilized in designing of

the shell and tube heat exchanger. The decrease in entropy (caused by fluid's friction) makes a drastic decrease in the pumping power of two heat exchangers from 51.4 to 82.2 percent and 54.8 to 92.2 percent, respectively.

Mohanty [12] have optimized two shell and tube heat exchangers with thermal capacities of 4.34 and 1.44 Megawatts with considering the total cost as the objective function, and through the firefly algorithm. The total cost consists of an initial cost and operation cost. Their result for the 4.34, and 1.44 Megawatt heat exchangers was 27.4 percent, and 8 percent decrease for the heat exchanger area and 29 percent, and 28 percent decrease in the total cost, respectively. Pu et al. [13] have optimized the design parameters of a ground heat exchanger for a ground-source heat pump through a multi-objective genetic algorithm mixed with the Kriging interpolation.

In this research, the effect of the design parameters on the entropy production rate was investigated. The investigated design parameters were the inflow velocity, inflow temperature, the U-shaped tube diameter, the channel diameter, and tubes distances. Mirzaei et al. [14] have accomplished the optimization of the efficacy and the cost parameters in a shell and tube heat exchanger through a multi-objective optimization method with two objective functions of maximizing the efficacy and minimizing the cost. Thermal efficiency has increased by nearly 28 percent by mixing the genetic algorithm with constructal theory. Zarea et al. [15] have optimized a plate-fin heat exchanger by considering 7 parameters of optimization (the hot and cold inflow length, number of fin layers, fin frequency, fin height, fin length, and fin thickness) and by maximizing the efficacy of the exchanger and minimizing the entropy production through the  $\epsilon$ -NTU method and the bees algorithm. They have demonstrated that the utilization of the bees algorithm in the optimization of the plate-fin heat exchanger is efficient.

Etghani et al. [16] have carried out the optimization of four significant parameters of coil pitch, tube diameter, hot and cold inflow rate in the design of a shell and tube heat exchanger through the Taguchi Method for achieving the maximum heat transfer coefficient and minimum exergy loss. Their results depict that the maximum Nusselt number has been observed in the maximum hot and cold inflows and the heat transfer coefficient has increased by increasing the coil pitch and the hot inflow rate. Yang et al. [17] have optimized a serrated fin-plate heat exchanger by considering five important parameters of design (fin height, fin distance, fin thickness and length, and the Reynolds number of the channel). The objective functions were the heat transfer rate, total annual cost, and entropy production, and the optimization process was made through the Morris and Sobol sensitivity analysis and non-dominated ranking

genetic algorithm. Their results illustrate the fact that Reynold's number and fin distance play a significant role in the performance of the serrated plate-fin heat exchanger. Many studies that address the heat exchanger design using optimization algorithms have achieved design parameters by disregarding the sensitivity of these parameters to objective functions. However, this study earmarks the sensitivity of the design parameters to heat transfer and pressure drop to uncover more optimal solutions. In the current study, the structural design optimization of the gasketed-plate heat exchanger (GPHE), presented in “Fig. 1” has been studied with the stated characteristics in “Table 1”, and for the cold water heating purpose through a combination of thermal-hydraulic modeling and bees optimization algorithm. The procedure of the bees optimization algorithm and the related equations for the design and optimization of the heat exchanger are discussed in the following sections.

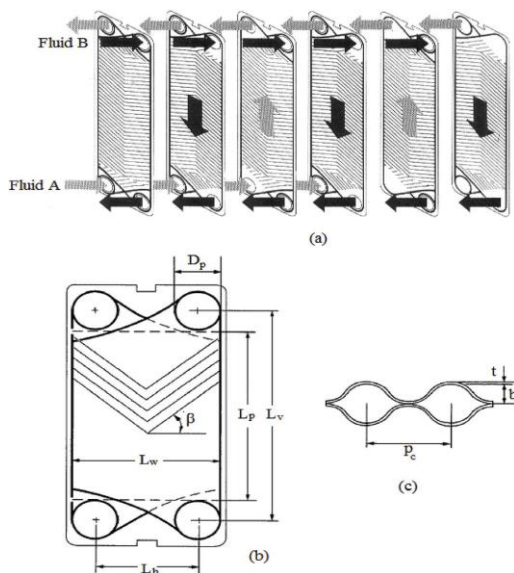


Fig. 1 Simple schematic of a gasketed-plate heat exchanger.

Table 1 Geometric characteristics of the gasketed-plate heat exchanger [19]

Plate thickness ( <i>t</i> )	0.6 mm
Chevron angle ( $\beta$ )	45°
Total number of plates ( $N_t$ )	105
Enlargement factor ( $\phi$ )	1.25
Number of passes	One pass/one pass
Total effective area ( $A_e$ )	110 m <sup>2</sup>
All port diameter ( $D_p$ )	200 mm
Effective channel width ( $L_w$ )	0.63m
Vertical port distance ( $L_v$ )	1.55 m
Horizontal port distance ( $L_h$ )	0.43 m
Compressed plate pack length ( $L$ )	0.38 m
Thermal conductivity of the plate material ( $k_w$ )	17.5 W/m.K

## 2 THE BEES ALGORITHM

The bees algorithm is a population-based search algorithm that has been developed by Pham et al. [18]. In this method, n number of bees are in search of a food/flower source (the solution of the problem) and each time that an artificial bee reaches the flower, the profit is evaluated. The bees possess this ability to improve the solution and find better ones by utilizing the others' information. This algorithm can be used to solve problems that have many solutions, some of which are better than other. So that, it starts with a random solution, and iteratively makes small changes to the solution, each time improving it a little. When the algorithm cannot see any improvement anymore, it terminates.

## 3 MODELING FORMULATION

This section describes thermal-hydraulic modelling of GPHE, objective function formulation, design variables, and constraints involved in GPHE design optimization.

### 3.1. Thermal and Hydraulic Formulation

In this work, the GPHE is assumed to run under a steady state, with negligible heat loss and uniform velocities. Further, heat transfer coefficients are assumed to be uniform and constant.

#### 3.1.1. Heat Transfer

The hot water at 338 K is entering into GPHE with the mass flow rate of 140 kg/s. The cold water having the mass flow rate of 140 kg/s is supplied to GPHE at a temperature of 295 K. The transferred heat exchange in the GPHE can be calculated as follows [19]:

$$Q_f = U_f A_e \Delta T_m \tag{1}$$

$A_e$  is the total developed area of all thermally effective plates, and  $\Delta T_m$  is the mean temperature difference. In “Eq. (1)”, the fouled (service) overall heat transfer coefficient is calculated based on the following, and the value of 0.00005 m<sup>2</sup>.K/W in (“Eq. (2)”) is the fouling factor [19]:

$$U_f = \left( \frac{1}{U_c} + 0.00005 \right)^{-1} \tag{2}$$

In “Eq. (2)”, the overall heat transfer coefficient for a clean surface can be calculated by:

$$U_c = \left( \frac{1}{h_c} + \frac{1}{h_h} + \frac{t}{k_w} \right)^{-1} \tag{3}$$

In “Eq. (3)”,  $t$  and  $k_w$  are the plate thickness and plate thermal conductivity, respectively, and the heat transfer coefficients for both hot and cold flows are calculated by considering the thermo-physical properties of hot and cold water, which is presented in “Table 2” as follows:

**Table 2** Thermophysical properties of hot and cold water

Property	Water (hot stream)	Water (Cold stream)
$c_p$ [J kg <sup>-1</sup> K <sup>-1</sup> ]	4183	4178
$\rho$ [kg m <sup>-3</sup> ]	985	995
$k$ [Wm <sup>-1</sup> K <sup>-1</sup> ]	0.645	0.617
$\mu$ [kg m <sup>-1</sup> s <sup>-1</sup> ]	$5.09 \times 10^{-4}$	$7.66 \times 10^{-4}$

$$h = \frac{ck}{D_h} \text{Re}^n \text{Pr}^{\frac{1}{3}} \quad (4)$$

Where:

$$\text{Re} = \left( \frac{\dot{m} / N_{cp}}{A_{ch}} \right) \frac{D_h}{\mu} \quad (5)$$

$$\text{Pr} = \frac{c_p \mu}{k} \quad (6)$$

In “Eq. (4)”,  $c$  and  $n$  values for  $Re > 100$  and  $\beta = 45^\circ$  are 0.3 and 0.663, respectively. In “Eq. (5)”,  $N_{cp}$ ,  $D_h$  and  $A_{ch}$  are the number of channels in each passage, the hydraulic diameter of channel and the one channel flow area, respectively, which can be given as:

$$N_{cp} = \frac{N_t - 1}{2N_p} \quad (7)$$

$$D_h = \frac{2b}{\phi} \quad (8)$$

$$A_{ch} = bL_w \quad (9)$$

In “Eq. (7)”,  $N_p$  is equal to 1 for one pass in tubes, and also  $N_t$  is the total number of plates. In “Eq. (8)”,  $\phi$  and  $b$  are the enlargement factor and the channel depth, respectively, which can be given as:

$$\phi = \frac{(A_e / N_e)}{L_p \times L_w} \quad (10)$$

$$p = \frac{L}{N_t}, b = p - t \quad (11)$$

In “Eq. (10)”,  $N_e$  is the effective number of plates that is equal to  $N_t - 2$  and  $L_p$  is equal to  $L_v - D_p$  considering the “Fig. 1”. In “Eq. (11)”,  $p$  is the plate pitch and  $L$  is the compressed plate pack length.

### 3.1.2. Pressure Drop

The total pressure drop of GPHE is equal to the total pressure drops of channels and ports. Thus [20]:

$$\Delta P_{total} = \Delta P_{channel} + \Delta P_{port} \quad (12)$$

Where:

$$\Delta p_{channel} = 4f \frac{L_v N_p}{D_h} \frac{\dot{m}^2}{2N_{cp}^2 A_{ch}^2 \rho} \quad (13)$$

$$\Delta p_{port} = 11.2 N_p \frac{\dot{m}^2}{\rho \pi^2 D_p^4} \quad (14)$$

In “Eq. (13)”, the fluid friction coefficient for  $Re > 300$ , and  $\beta = 45^\circ$  is equal to:

$$f = \frac{1.441}{\text{Re}^{0.206}} \quad (15)$$

Also, the pumping power is calculated by the overall pressure drop:

$$PP = \Delta p_{total} \times \left( \frac{\dot{m}}{\rho} \right) \quad (16)$$

### 3.2. Objective Function and Design Variables and Constraints

In the present study, the optimization of the GPHE with the objective function of heat exchanger performance index (the ratio of transferred heat exchange to pumping power,  $\eta = Q_f / PP$ ), and by considering 6 design parameters (the port diameter, plate thickness, the enlargement factor, the compressed plate pack length, the horizontal port distance, and the vertical port distance) is made through the bees algorithm. The population (number of bees) is 25, and the iteration number is 100 for the optimization algorithm. The boundaries of design parameters that have been utilized in the heat exchanger are presented in “Table 3”.

**Table 3** Design parameters and corresponding ranges

Decision Variables	Range
$D_p$ (m)	0.1-0.3
$t$ (m)	0.0003-0.001
$\phi$	1.15-1.25
$L$ (m)	0.3-0.6
$L_h$ (m)	0.3-0.7
$L_v$ (m)	1.1-2

### 4 RESULTS AND DISCUSSION

The two sets of optimized solutions from the collection of bees algorithm optimized solutions have been chosen as the most suitable design parameters of the GPHE, and they have been compared to the design parameters of Kakac et al. [19]. By choosing the optimized design parameters of solution collection (1), presented in “Table 4” , in comparison to Kakac et al. [19], the transferred heat exchange, pumping power are decreased by 2.77 percent, and 83.41 percent, respectively; furthermore, the performance index of the heat exchanger is increased by 5.68.

**Table 4** The comparison between the results obtained by BA and the corresponding results from reference [19]

	Reference [19]	BA (1)	BA (2)
$D_p(m)$	0.2	0.20127	0.14355
$t(m)$	0.0006	0.00057499	0.0006805
$\phi$	1.55	1.1509	1.2498
$L(m)$	0.38	0.59408	0.38156
$L_h(m)$	0.43	0.6592	0.69021
$L_v(m)$	1.55	1.7565	1.7459
Q (KW)	16658	16196	23585
pp (W)	39738	6591.7	35013
$\eta$	419.18	2457.1	673.62

Also, by choosing the optimized design parameters of solution collection (2), in comparison to Kakac et al. [19], the transferred heat exchange is increased by 41.6 percent, the pumping power is decreased by 11.89 percent, and the performance index of the heat exchanger is increased by 1.6. Therefore, the designer of the heat exchanger can choose the optimized design parameters based on the requirements of the corresponding unit for purposes of either increasing the transferred heat exchange or the pumping power decrease. Almost always, the approaches of increasing the transferred heat exchange in the heat exchangers are leading to the pumping power increase. We have depicted that by proper optimizing of the GPHE, the transferred heat exchange can be increased without the tangible increase of the pumping power. Besides, to explore the feasibility of attaining a more optimal heat exchanger, the present study probes the sensitivity of the design parameters considered in the optimization of the GPHE to the objective functions, including the rates of heat exchange and pump power. In this regard, these parameters are considered constant in the marked range, and other parameters are considered variable.

#### 4.1. The Impact of the Enlargement Factor On the Optimization Process

By considering the constant enlargement factor values in the range of  $1.15 \leq \phi \leq 1.25$ , the effect of this parameter on the amount of transferred heat exchange and pumping

power, (and therefore, the heat exchanger performance index) has been evaluated. The evaluation includes the other five design parameters as variables and is made through the bees algorithm. The results are demonstrated in “Fig. 2” , and they depict an increase in the amount of transferred heat exchange and pumping power, and the heat exchanger performance index, with an increase in the enlargement factor.

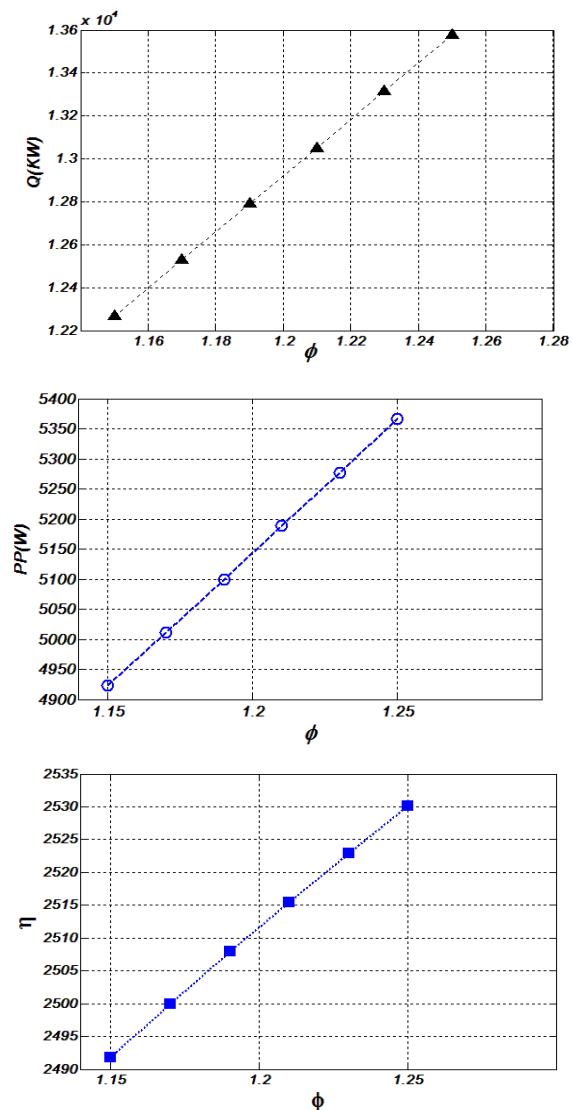


**Fig. 2** The impact of the enlargement factor on heat transfer rate, pumping power and performance index.

In the optimization process, and various values of the enlargement factor (1.15, 1.17, 1.19, 1.21, 1.23, and 1.25), the values of the other five parameters are the same, in the best heat exchanger performance index among this evaluation. These values are presented in “Table 5” , and they illustrate that the amount of transferred heat exchange and pumping power, and the heat exchanger performance index in  $\phi=1.25$ , in

proportion to  $\phi=1.15$  has increased by 10.66 percent, 8.98 percent, and 1.53 percent, respectively. Thus, it can be concluded that the heat exchanger performance index in this optimization process (the constant enlargement factor) has not been increased noticeably, and is not desirable. Likewise, despite a suitable reduction in the pump power, the constancy of the magnification factor design parameter is not recommended in the optimization process of the GPHE due to the decline of heat transfer compared to the heat exchanger designed by Kakac et al. [19].

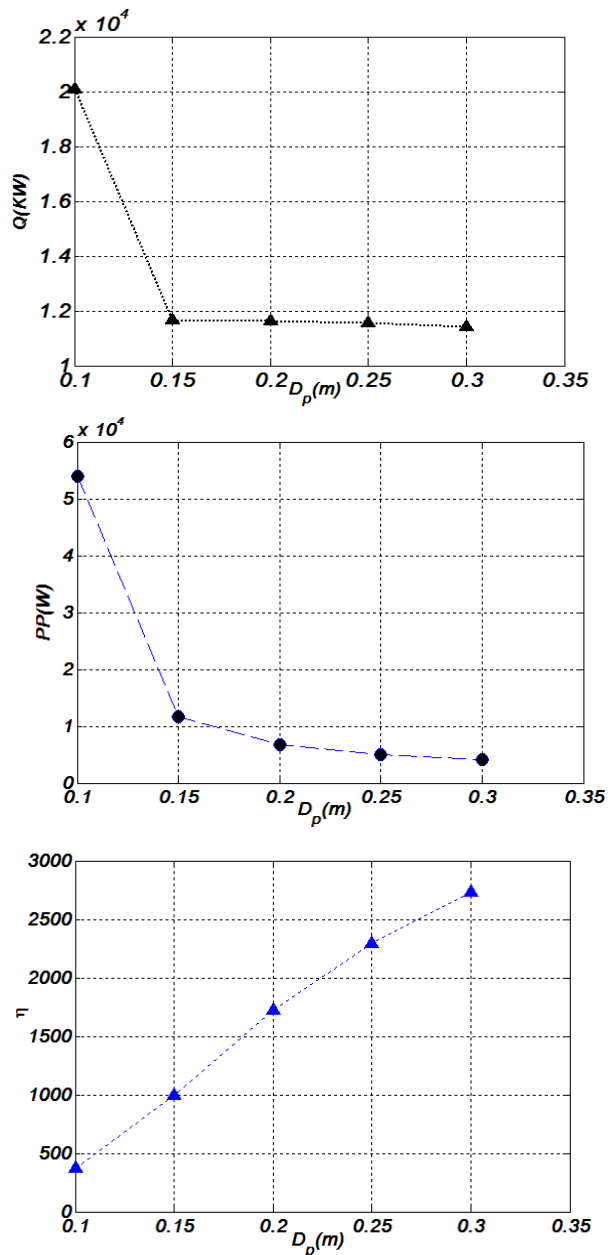


Fig. 3 The impact of the port diameter on heat transfer rate, pumping power and performance index.

Table 5 The optimal variables in the optimization process at different enlargement factor

$L_v$ (m)	$L_h$ (m)	$L$ (m)	$t$ (m)	$D_p$ (m)
1.478	0.54019	0.59663	0.00048	0.25652

#### 4.2. The Impact of the Port Diameter on the Optimization Process

Based on “Fig. 3”, the rates of heat transfer and pump power approximately decrease by 43.13% and 92.27% as the port diameter increases from 0.1 m to 0.3 m. When the port diameter is considered constant at 0.1 m in the optimization process, and the other design parameters are considered variable, compared to the heat exchanger designed by Kakac et al. [19], the heat transfer and pump power rates increase by 20.51% and 3.6%, indicating a desirable result. However, by choosing the optimal design parameters of the solution set (2), illustrated in “Table 4” and obtained when the six design parameters were variable; e.g., the port diameter, we can decrease heat transfer and pump power by 41.6% and 11.89% and yield much more suitable results. The maximum rates of heat transfer and pump power were observed when the port diameter was constant at 0.1 m, and the heat transfer and pump power variations were smaller when the port diameter increased from 0.15 to 0.3 m. Also, the rates of heat transfer and pump power were smaller than those in the GPHE designed by Kakac et al. [19]. The optimized values of the other five parameters for various port diameters are displayed in Table 6. Moreover, it has been noticed that for various values of the port diameter, the optimized other five parameters values are the same; except in  $D_p=0.1$  m case.

Table 6 The optimal variables in the optimization process at different port diameter

$D_p$ (m)	$L_v$ (m)	$L_h$ (m)	$L$ (m)	$t$ (m)	$\phi$
0.1	1.8454	0.65591	0.44378	0.00085	1.1869
0.15, 0.2, 0.25, 0.3	1.3253	0.55031	0.59941	0.00058	1.2307

#### 4.3. The Impact of the Plate Thickness on the Optimization Process

Based on the “Fig. 4”, by increasing the plate thickness from 0.3 mm to 1 mm, the transferred heat exchange amount, and the heat exchanger performance index are decreased by 9.31 percent, and 36.82 percent, respectively, and the pumping power is increased by 43.55 percent. Thus, the constancy of this design parameter in the optimization process of the GPHE is not recommended. All of the other five optimized design parameters are the same, and they are presented in “Table 7”. By comparing “Table 7 to Table 5”, or the

optimized values of the constant plate thickness to the optimized values of the constant enlargement factor, it is unrevealed that the design parameters of  $D_p$ ,  $L$ ,  $L_h$  and  $L_v$  possess the same optimized values for maximizing the heat exchanger performance index.

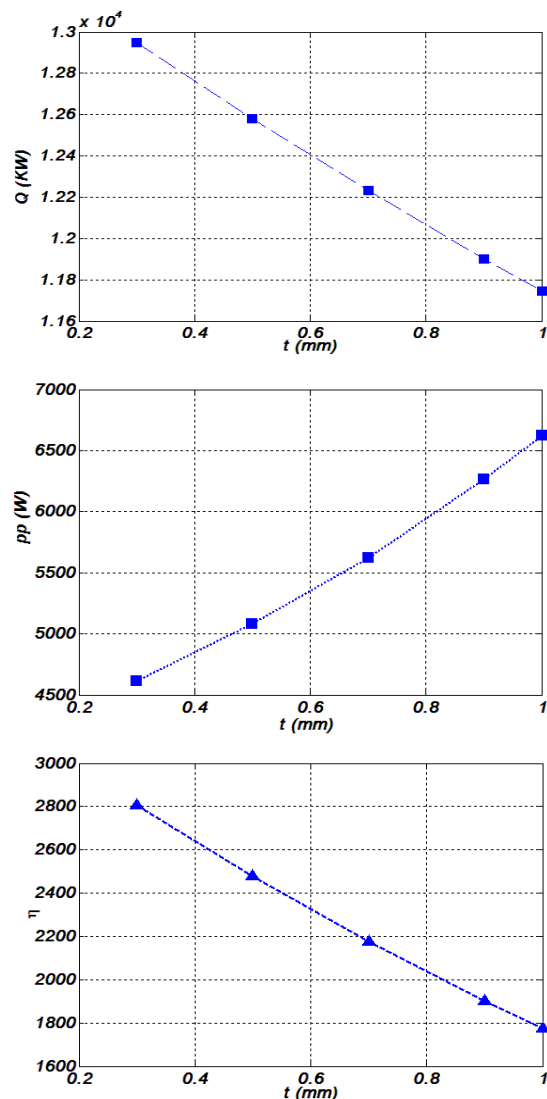


Fig. 4 The impact of the plate thickness on heat transfer rate, pumping power and performance index.

Table 7 The optimal variables in the optimization process at different plate thickness

$L_v$ (m)	$L_h$ (m)	$L$ (m)	$\phi$	$D_p$ (m)
1.478	0.54019	0.59663	1.1762	0.25652

#### 4.4. The Impact of the Compressed Plate Pack Length On the Optimization Process

According to “Fig. 5”, by increasing the compressed plate pack length (heat exchanger length) from 0.3 m to 0.6 m, the heat exchanger performance index has been increased by nearly five times; even by the 37 percent

decrease in the transferred heat exchange amount. This amount of increase is due to the significant decrease (87.95 percent) in the pumping power. Also, the results show that the heat transfer rate increases by 34.55% and the pump power decreases by 27% when the compressed plate pack length is constant in 0.3m, and other design parameters are variable compared to the GPHE designed by Kakac et al. [19]; revealing very desirable results. All of the other five optimized design parameters are the same, and they are displayed in “Table 8” .

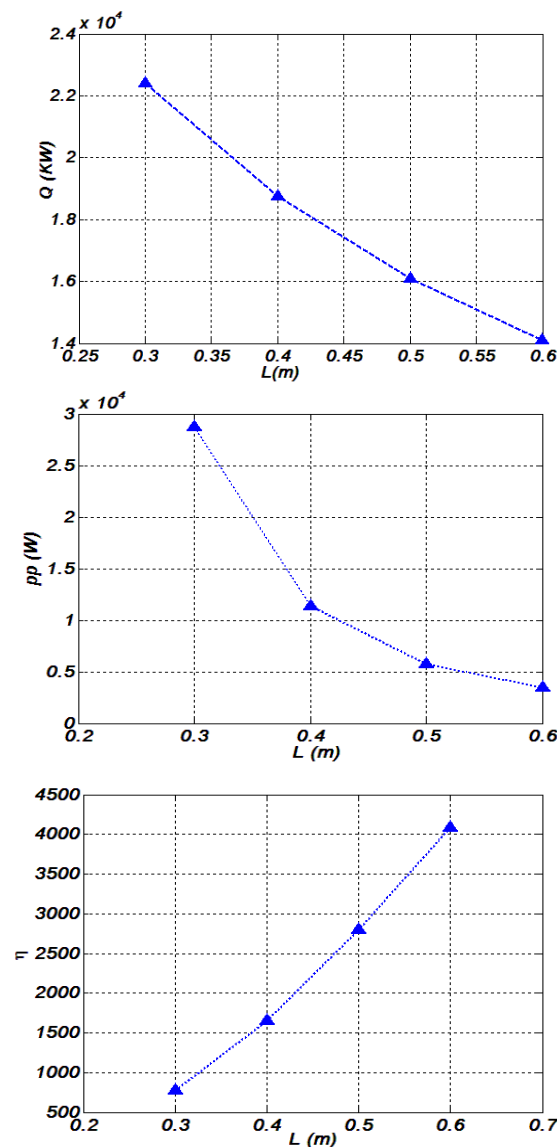


Fig. 5 The impact of the heat exchanger length on heat transfer rate, pumping power and performance index.

Table 8 The optimal variables in the optimization process at different heat exchanger length

$L_v$ (m)	$L$ (m)	$t$ (m)	$\phi$	$D_p$ (m)
1.5066	0.57857	0.00033	1.1699	0.27458

#### 4.5. The Impact of the Horizontal Port Distance On the Optimization Process

It has been illustrated in “Fig. 6” that by fixing the horizontal port distance in the range of 0.3 m to 0.7 m, and 5 other variable design parameters in optimization process, the heat exchanger performance index has been increased about three times (due to 34.88 percent increase in the transferred heat exchange amount, and 57.2 percent decrease in the pumping power).

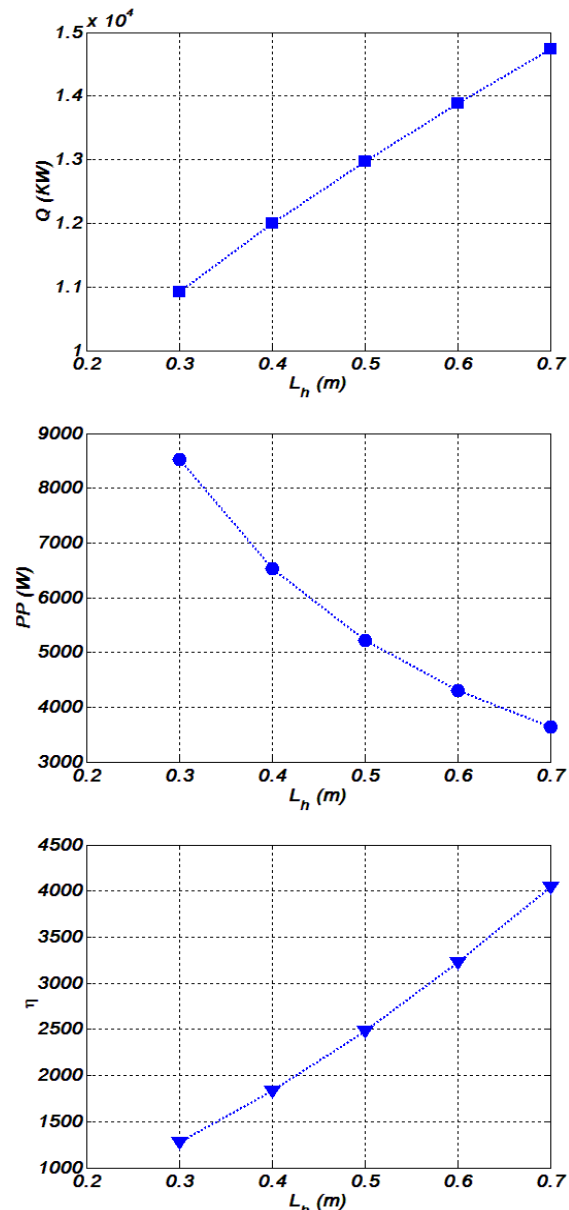


Fig. 6 The impact of the horizontal port distance on heat transfer rate, pumping power and performance index.

However, since the values obtained for the exchanged heat transfer are smaller than those obtained from the GPHE designed by Kakac et al. [19], the constancy of the horizontal port distance is not suggested contrary to

the suitable reduction in the pump power. For all of the values in range, all of the other five optimized design parameters are the same, and they are displayed in “Table 9” . By comparing “Table 9 to Table 8” , or the optimized values of the constant heat exchanger length to the optimized values of the constant horizontal distance between the ports, it has been proven that the design parameters of  $D_p$ ,  $t$ ,  $\phi$ , and  $L_v$  possess the same optimized values for maximizing the heat exchanger performance index.

Table 9 The optimal variables in the optimization process at different horizontal port distance

$L_v$ (m)	$L_h$ (m)	$t$ (m)	$\phi$	$D_p$ (m)
1.5066	0.67143	0.00033	1.1699	0.27458

#### 4.6. The Impact of the Vertical Port Distance on the Optimization Process

As it has been displayed in “Fig. 7” , by fixing the vertical port distance in the range of 1.1 m to 2 m, and 5 other variable design parameters in the optimization process, the heat exchanger performance index has been increased by about 23.67 percent (due to the doubling in the transferred heat exchange amount, and 67.44 percent decrease in the pumping power). The results show that the heat transfer rate increases by 20.7%, and pump power decreases by 83% when the vertical port distance is equal to 2m in the optimization process, and other design parameters are variable, compared to the GPHE designed by Kakac et al. [19]. These values indicate very desirable results. For all of the values in range, all of the other five optimized design parameters are the same, and they are displayed in “Table 10” .

Table 10 The optimal variables in the optimization process at different vertical port distance

$L_h$ (m)	$L$ (m)	$t$ (m)	$\phi$	$D_p$ (m)
0.63128	0.56693	0.00055	1.1979	0.25967

Table 11 The optimal solution sets of design parameters.

	$L_v$ (m)	$L_h$ (m)	$L$ (m)	$\phi$	$t$ (m)	$D_p$ (m)
1	1.7459	0.690 21	0.381 56	1.24 98	0.00068 05	0.143 55
2	1.5066	0.671 43	0.3	1.16 99	0.00033 955	0.274 58
3	2	0.631 28	0.566 93	1.19 79	0.00055 815	0.259 67

#### 4.7. The Suggested Optimal Solution Sets of Design Parameters

Concerning the posed subjects, the present study proposes three suitable solution sets for the optimization of the GPHE designed by Kakac et al. [19] and presents them in “Table 11” . The design parameters in these three optimal solution sets were opted in such a way that

heat transfer increased by 41.6%, 34.55%, and 20.7%, and pressure drop decreased by 11.89%, 27%, and 83%, respectively.

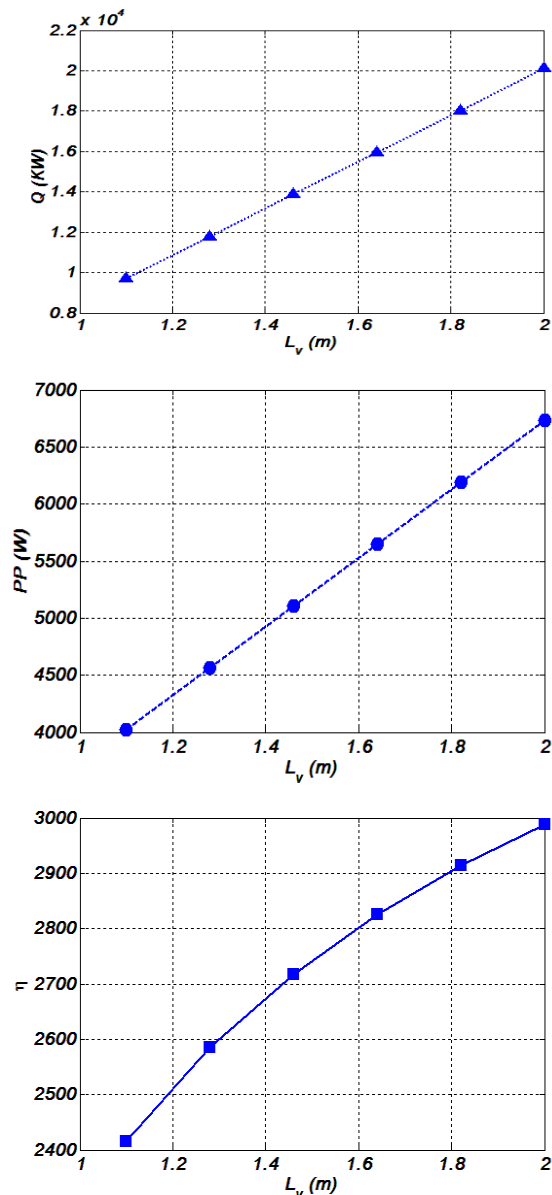


Fig. 7 The impact of the vertical port distance on heat transfer rate, pumping power and performance index.

## 5 CONCLUSIONS

The heat exchange increase in the heat exchangers is usually followed by a significant increase in pressure drop. In the present study, six design parameters (the port diameter, plate thickness, the enlargement factor, the compressed plate pack length, the horizontal port distance, and the vertical port distance) by considering the heat exchanger performance index (the amount of

transferred heat exchange to the pumping power) as the objective function through the bees algorithm have been modified and optimized. Also, the effect of these parameters on the performance of a gasketed-plate heat exchanger has been evaluated and analyzed singularly, to choose the suitable values of the parameters. Finally, three optimal solution sets were selected from the output solution sets of the bee algorithm for the design parameters in the optimization process of the GPHE. The heat transfer rate can increase by 41.6%, 34.55%, and 20.7%, and pressure drop can decrease by 11.89%, 27%, and 83%, respectively, when every one of these solution sets is selected.

## NOMENCLATURE

$A_e$	Total effective area, $m^2$
$A_{ch}$	Channel flow area, $m^2$
$b$	Channel flow gap, m
$c_p$	Specific heat of fluid, J/kg. K
$D_p$	Port diameter, m
$f$	Fanning friction factor
$h$	Heat transfer coefficient, $W/m^2K$
$k$	Thermal conductivity, W/m. k
$L$	Compressed plate pack length, m
$L_h$	Horizontal port distance, m
$L_p$	Projected plate length, m
$L_v$	Vertical port distance, m
$L_w$	Plate width inside gasket, m
$\dot{m}$	Mass flow rate, kg/s
$N_{cp}$	Number of channels in each passage
$N_e$	Effective number of plate
$N_p$	Number of passes
$N_t$	Total number of plates
$p$	Plate pitch, m
$Pr$	Prandtl number
$Q_f$	Heat load under fouled conditions, W
$Re$	Reynolds number
$t$	Plate thickness, m
$U_c$	Clean overall heat transfer coefficient, $W/m^2. K$
$U_f$	Fouled (service) overall heat transfer coefficient, $W/m^2. K$

## Greek Symbols

$\beta$	chevron angle, deg
$\rho$	fluid density, $kg/m^3$
$\phi$	enlargement factor
$\mu$	viscosity, kg/ms

## Subscripts

$c$	cold fluid
$h$	hot fluid
$w$	wall

**REFERENCES**

- [1] Wang, C., Cui, Z., Yu, H., Chen, K., and Wang, J., Intelligent Optimization Design of Shell and Helically Coiled Tube Heat Exchanger Based On Genetic Algorithm, *International Journal of Heat and Mass Transfer*, Vol. 159, 2020. DOI: 10.1016/j.ijheatmasstransfer.2020.120140.
- [2] Zhicheng, Y., Lijun, W., Zhaokuo, Y., and Haowen, L., Shape Optimization of Welded Plate Heat Exchangers Based On Grey Correlation Theory, *Applied Thermal Engineering*, Vol. 123, 2017, pp. 761-769. DOI: 10.1016/j.appltherm.aleng.2017.05.005.
- [3] Maghsoudi, P., Sadeghi, S., and Gorgani, H. H., Comparative Study and Multi-Objective Optimization of Plate-Fin Recuperators Applied in 200 kW Microturbines Based On Non-Dominated Sorting and Normalization Method Considering Recuperator Effectiveness, Exergy Efficiency and Total Cost, *International Journal of Thermal Sciences*, Vol. 124, 2018, pp. 50-67, DOI: 10.1016/j.ijthermalsci.2017.10.001.
- [4] Hasanpour, A., Farhadi, M., and Sedighi, K., Intensification of Heat Exchangers Performance by Modified and Optimized Twisted Tapes, *Chemical Engineering & Processing: Process Intensification*, Vol. 120, 2017, pp. 276-285, DOI: 10.1016/j.cep.2017.07.026.
- [5] Zhang, P., Ma, T., Li, W. D., Ma, G. Y., and Wang, Q. W., Design and Optimization of a Novel High Temperature Heat Exchanger for Waste Heat Cascade Recovery from Exhaust Flue Gases, *Energy*, Vol. 160, 2018, pp. 3-18, DOI: 10.1016/j.energy.2018.06.216.
- [6] Wang, S., Jian, G., Xiao, J., Wen, J., Zhang, Z., and Tu, J., Fluid-Thermal-Structural Analysis and Structural Optimization of Spiral-Wound Heat Exchanger, *International Communications in Heat and Mass Transfer*, Vol. 95, 2018, pp. 42-52. DOI: 10.1016/j.ich.heatmasstransfer.2018.03.027.
- [7] Wang, C., Zhengyu, C., Hongmei, Y., Kai, C., and Jianli, W., Intelligent Optimization Design of Shell and Helically Coiled Tube Heat Exchanger Based On Genetic Algorithm, *International Journal of Heat and Mass Transfer*, Vol. 159, 2020. DOI: 10.1016/j.ijheatmasstransfer.2020.120140.
- [8] Yin, Q., Du, W. J., Ji, X. L., and Cheng, L., Optimization Design and Economic Analyses of Heat Recovery Exchangers On Rotary Kilns, *Applied Energy*, Vol. 180, 2016, pp. 743-756. DOI: 10.1016/j.apenergy.2016.07.042.
- [9] Momeni, S. M., Salehi, G., and Eshagh Nimvari, M., Modeling and Thermoeconomic Optimization of Marine Diesel Charge Air Cooler, *Energy*, Vol. 162, 2018, pp. 753-763. DOI: 10.1016/j.energy.2018.08.092.
- [10] Wu, J., Liu, S., and Wang, M., Process Calculation Method and Optimization of the Spiral-Wound Heat Exchanger with Bilateral Phase Change, *Applied Thermal Engineering*, Vol. 134, 2018, pp. 360-368. DOI: 10.1016/j.applthermaleng.2018.01.128.
- [11] Omolayo Petinrin, M., Bello-Ochende, T., Adebukola Dare, A., and Olanrewaju Oyewola, M., Entropy Generation Minimisation of Shell-and-Tube Heat Exchanger in Crude Oil Preheat Train using Firefly Algorithm, *Applied Thermal Engineering*, Vol. 145, 2018, pp. 264-276. DOI: 10.1016/j.applthermaleng.2018.09.045.
- [12] Mohanty, D. K., Application of Firefly Algorithm for Design Optimization of a Shell and Tube Heat Exchanger from Economic Point of View, *International Journal of Thermal Sciences*, Vol. 102, 2016, pp. 228-238. DOI: 10.1016/j.ijthermalsci.2015.12.002.
- [13] Pu, L., Qi, D., Xu, L., and Li, Y., Optimization on the Performance of Ground Heat Exchangers for GSHP Using Kriging Model Based on MOGA, *Applied Thermal Engineering*, Vol. 118, 2017, pp. 480-489. DOI: 10.1016/j.applthermaleng.2017.02.114.
- [14] Mirzaei, M., Hajabdollahi, H., Fadakar, H., Multi-Objective Optimization of Shell-And-Tube Heat Exchanger by Constructal Theory, *Applied Thermal Engineering*, Vol. 125, 2017, pp. 9-19. DOI: 10.1016/j.applthermal.Eng.2017.06.137.
- [15] Zarea, H., Kashkooli, F. M., Mehryan, A. M., Saffarian, M. R., and Beherghani, E. N., Optimal Design of Plate-Fin Heat Exchangers by a Bees Algorithm, *Applied Thermal Engineering*, Vol. 69, 2014, pp. 267-277. DOI: 10.1016/j.applthermaleng.2013.11.042.
- [16] Etghani, M., Hosseini Baboli, S. A., Numerical Investigation and Optimization of Heat Transfer and Exergy Loss in Shell and Helical Tube Heat Exchanger, *Applied Thermal Engineering*, Vol. 121, 2017, pp. 294-301. DOI: 10.1016/j.applthermaleng.2017.04.074.
- [17] Yang, H., Wen, J., Wang, S., Li, Y., Thermal Design and Optimization of Plate-Fin Heat Exchangers Based Global Sensitivity Analysis and NSGA-II, *Applied Thermal Engineering*, Vol. 136, 2018, pp. 444-453. DOI: 10.1016/j.applthermaleng.2018.03.035.
- [18] Pham, D. T., Ghanbarzadeh, A., Koc, E., Otri, S., Rahim, S., and Zaidi, M., The Bees Algorithm. Technical Note, Manufacturing Engineering Centre, Cardiff University, UK, 2005.
- [19] Kakac, S., Liu, H., Heat Exchangers Selection, Rating, and Thermal Design, Boca Raton London New York Washington, D. C., 2002.
- [20] Cao, E., Heat Transfer in Process Engineering, New York: McGraw-Hill, 2010.